Arch. Metall. Mater. **69** (2024), 2, 747-752

DOI: https://doi.org/10.24425/amm.2024.149806

N.A.Z. ZAITON[1], N. PARIMIN[1,2*], N.F. HAYAZI[1,2], F.F. ZAINAL[1,2], S. GARUS[3], P. VIZUREANU[4]

EFFECT OF HEAT TREATMENT TEMPERATURE ON ISOTHERMAL OXIDATION OF Ni-BASED Fe-33Ni-19Cr ALLOY

This project studies the influence of different grain sizes of Ni-based Fe-33Ni-19Cr alloy obtained from heat treatment procedure on high temperature isothermal oxidation. Heat treatment procedure was carried out at two different temperatures, namely 1000°C and 1200°C for 3 hours of soaking time, followed by quenching in the water. These samples are denoted as T1000 and T1200. The heat-treated Ni-based Fe-33Ni-19Cr alloy was subjected to an isothermal oxidation test at 950°C for 150 hours exposure. Oxidized heat-treated alloys were tested in terms of oxidation kinetics, phase analysis and surface morphology of oxidized samples. Oxidation kinetics were determine based on weight change per surface area as a function of exposure time. Phase analysis was determined using the x-ray diffraction (XRD) technique and surface morphology of oxidized samples was characterized using a scanning electron microscope (SEM). As a result, the heat treatment procedure shows varying grain sizes. The higher the heat treatment temperature, shows an increase in grain size with a decrease in hardness value. The oxidation kinetics for both heat-treated samples showed an increment pattern of weight change and followed a parabolic rate law. The oxidized T1000 sample recorded the lowest parabolic rate constant of 3.12×10^{-8} $mg^2cm^{-4}s^{-1}$, indicating a low oxidation rate, thus having good oxidation resistance. Phase analysis from the XRD technique recorded several oxide phases consisting of Cr_2O_3, $MnCr_2O_4$, and $(Ti_{0.97}Cr_{0.03})O_2$ oxide phases. In addition, a uniform oxide layer is formed on the oxidized T1000 sample, indicating good oxide scale adhesion, thereby improving the protective oxide behavior.

Keyword: Ni-based Alloys; Fe-Ni-Cr Alloys; Incoloy 800H Alloy; High Temperature Oxidation; Oxidation Kinetics

1. Introduction

Ni-based alloy have a variety of complex properties, including creep strength over width temperature range, high tensile and yield strength, and resistance to oxidation and corrosion [1-7]. Usually, high temperature oxidation and corrosion resistant Ni-based alloys are used at temperatures above 500°C [4-6]. The microstructure, thermal stability, and mechanical stability of Ni-based alloys were strongly influenced by the complex characteristic of this alloy [8]. Several alloying elements, were commonly added in alloy containing up to ten alloying elements [9-10]. Alloying method has been the dominant design technique for stabilizing compositions, microstructures, thermal properties and mechanical characteristics [8,11-13]. Because of its excellent high temperature oxidation resistance, and mechanical performance, Ni-based alloys have been widely used for production of component in hot stage conditions in the manufacture of aircraft engine, engine valves, gas turbine materials and chemical industry [2,4].

The ability of Ni-based alloys to resists oxidation in high temperature environments is mostly determined by their aptitude to form oxide scales that adhere specifically to metal surfaces. Maintains high adhesive oxide scale on heat resistant surfaces material is critical for long range oxidation resistance [14]. When subjected to high temperatures and harsh conditions, this alloys form oxide scales on the surface of the material. On the other hand, the presence of these oxides has the potential to slow the rate of oxidation and stop any further oxidation of the base material. In addition, oxide exfoliation was found to be a potentially dangerous process in prolonged service conditions, with the potential to cause significant structural damage [14].

On the other hand, the production of oxide scale is influenced by the exposure environment [15] as well as the oxidation temperature [16-17] and alloy composition [18-20].

[1] UNIVERSITI MALAYSIA PERLIS (UNIMAP), FACULTY OF CHEMICAL ENGINEERING & TECHNOLOGY, 02600 ARAU, PERLIS, MALAYSIA
[2] UNIVERSITI MALAYSIA PERLIS (UNIMAP), SURFACE TECHNOLOGY SPECIAL INTEREST GROUP, FACULTY OF CHEMICAL ENGINEERING & TECHNOLOGY, 02600 ARAU, PERLIS, MALAYSIA
[3] CZĘSTOCHOWA UNIVERSITY OF TECHNOLOGY, FACULTY OF MECHANICAL ENGINEERING AND COMPUTER SCIENCE, 42-201 CZĘSTOCHOWA, POLAND
[4] GHEORGHE ASACHI TECHNICAL UNIVERSITY OF IASI, FACULTY OF MATERIAL SCIENCE AND ENGINEERING, 41 D. MANGERON ST., 700050 IASI, ROMANIA

* Coressponding author: noraziana@unimap.edu.my

This is because the formation of the oxide phase is a complex process. The build-up has the potential to harm the component or prevent its function. In conclusion, the stability of oxide scale formation during oxidation is important to how this alloy behaves because it can increase scale adhesion and reduce scale exfoliation, which causes an oxide layer to form on the surface and protect it. Extensive research on high temperature oxidation investigates oxidation kinetics during oxide scale growth to further understand their behaviour. Oxide scale formation during the high temperature oxidation test is expressed in a plot of weight change per surface area versus exposure time. This plot shows the development of oxide scale during high temperature exposure at different temperature [21-22], alloy structure via different treatment parameter [23-24], exposure environment [25], composition [26-27].

The Ni-based Fe-33Ni-19Cr alloy is a heat-resistant alloy typically used at high temperatures. Upon exposure to high temperature conditions, a thin oxide layer is developed on the surface of the alloy which perform as a blockade between the environment and the alloy. Therefore, the alloy is protected by the oxide layer. However, during high temperature exposure and extended service time, oxide scale exfoliation may occur due to stress generation between the oxide layer and the alloy. This phenomenon will reduce the protective behavior of the oxide scale on the surface of the alloy. One possible method of reducing oxide exfoliation during service includes the use of fine-grained alloy. Fine-grained alloys are recorded to reduce the effect of oxide exfoliation and reduce oxidation rates [2,14,28]. One of the ways to obtain a fine grain size of the alloy is through a heat treatment procedure.

Therefore, in this study, a heat treatment procedure was implemented on the Ni-based Fe-33Ni-19Cr alloy to change the grain size. Then, alloys with different grain sizes accomplished from the heat treatment procedure were subjected to isothermal oxidation tests to investigate the oxidation behavior of the alloys.

2. Experiment

Ni-based Fe-33Ni-19Cr alloy was used in this study. Chemical composition was measured using optical emission spectroscopy (OES) technique. The chemical composition is recorded in weight percent (wt.%), consisting of 33 wt.% Ni, 19 wt.% Cr, 0.08 wt.% C, 0.05 wt.% Al, 0.49 wt.% Ti, 0.31 wt.% Si, 0.56 wt.% Mn and the rest Fe. This alloy is also known as Incoloy 800H alloy. The sample size used in this study is 10 mm × 10 mm × 3 mm.

The Fe-33Ni-19Cr alloy underwent a heat treatment procedure at two different temperatures namely 1000°C and 1200°C. The sample is held at the desired heat treatment temperature for 3 hours of soaking time followed by quenching in water. The two samples are designated as T1000 and T1200, respectively. The average grain size of the heat-treated samples was measured using the ASTM E112 method, which is the linear intercept method. The Rockwell hardness test is made to measure the hardness of heat-treated samples.

The heat-treated Fe-33Ni-19Cr alloy were underwent an isothermal oxidation test at temperatures of 950°C for 150 hours exposure time. The curve of the oxidation kinetics was projected based on the weight change per surface area as a function of time. The sample preparation for the oxidation test was conducted through a grinding method until the P600 grit surface finished. The initial weight and dimension measurement of each sample was documented prior the oxidation test. The isothermal exposure was done for selected interval duration of 30 hours. The final weight was determined after each interval of exposure duration. The oxidized samples were examined in terms of phase analysis using the x-ray diffraction (XRD) technique and surface morphology analysis using scanning electron microscope (SEM).

3. Results and discussion

3.1. Heat Treatment Procedure

Heat-treated samples T1000 and T1200 exhibit fine and coarse grain structures of 71.88 µm and 128.94 µm, respectively. These results shows that, as the heat treatment temperature increases, the grain structure is growth. Additionally, the Rockwell hardness test is inversely proportional to grain size. The hardness value decreases as the heat treatment temperature increases. The T1200 sample recorded a lower hardness value of 78.7 HRB, while the T1000 sample recorded a higher hardness value of 83.73 HRB. This finding is in line with previous studies, showing that when the heat treatment temperature increases, the average grain size will increase and the hardness value will decrease [29].

3.2. Oxidation Kinetics

Fig. 1 displays the oxidation kinetics of samples T1000 and T1200 after exposure for 150 hours expressed in a plot of weight change per surface area versus exposure time. Both samples showed a pattern of growing weight gain as the period of exposure increased. Similar weight gain curves were recorded for both samples from initial to 120 h exposure. Starting at 120 hours of exposure, the sample weight gain showed a slight

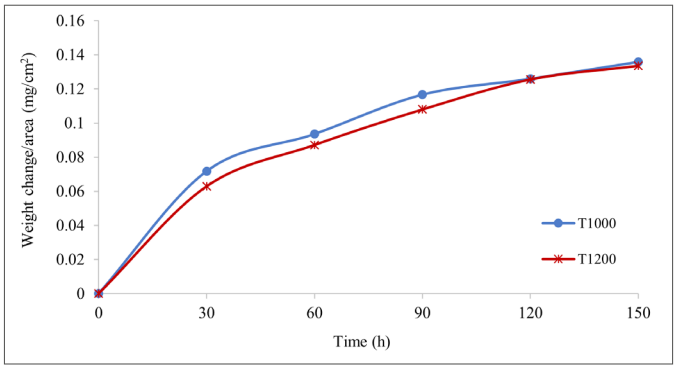

Fig. 1. Plot of weight change per surface area versus time during isothermal oxidation at 950°C for 150 h

decreasing trend, indicating a slower oxidation reaction. This downward trend in weight gain indicates formation the oxide layer begins to stabilize over a longer period of time. This trend is likely to resemble the parabolic rate law, whereas the exposure time of an alloy increases, the growth rate of the oxide layer begins to decrease. To find out the growth rate of the oxide layer, the determination of the oxidation rate law is done. The kinetics of this oxidation was further analyzed using a double log plot to identify the oxidation rate law of this sample, as shown in Fig. 2.

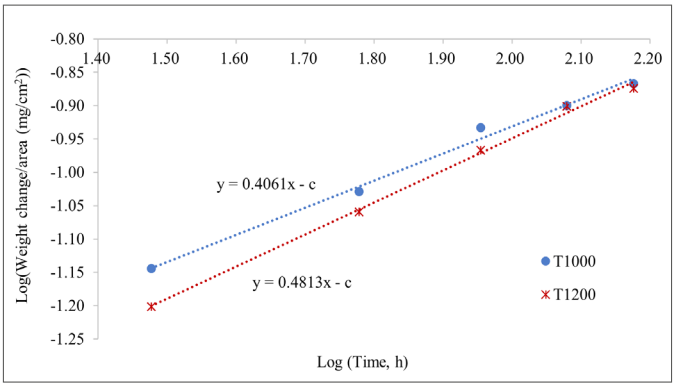

Fig. 2. A double log plot of weight change per surface area versus time indicating parabolic rate law (m = 2)

The oxidation rate law is calculated according to equation (1), where x is the weight change per surface area, t is time, c is constant and m shows the oxidation rate law. A quantity of m equivalent to 1 or 2 respectively indicates a linear or parabolic rate law. From Fig. 2, the curve analysis of both samples recorded m values equal to 2.46 and 2.08 for T1000 and T1200 samples, respectively. These results show that this sample follows a parabolic rate law. The parabolic rate law is supposed in this work because of their diffusion-controlled mechanism. As the oxidation time lengthens, the oxidation rate begins to decrease, increasing the optimum oxide scale thickness. The weight of the sample begins to plateau, developing good oxidation protection and preventing further forms of oxidation from occurring. This trend was also recorded from our previous study which showed a decrease in the oxidation rate as the exposure duration increased due to the diffusion-controlled mechanism from the parabolic rate phenomenon [2].

Fig. 3 displays the analysis of the parabolic rate law according to equation (2), where K_p is the parabolic rate constant. The T1000 sample exhibited a lower parabolic rate constant of 3.12×10^{-8} $mg^2cm^{-4}s^{-1}$, while the T1200 sample exhibited a higher parabolic rate constant of 3.33×10^{-8} $mg^2cm^{-4}s^{-1}$. Lower parabolic rate constant recorded by T1000 sample indicates a lower oxidation rate, therefore having good oxidation protection of the sample. On the other hand, the fine grain structure exhibits good oxidation protection by enhancing the optimal thickness of the protective oxide scale. Similar findings have been recorded by other researchers, with a refinement of the structure reduced the oxidation rate [28].

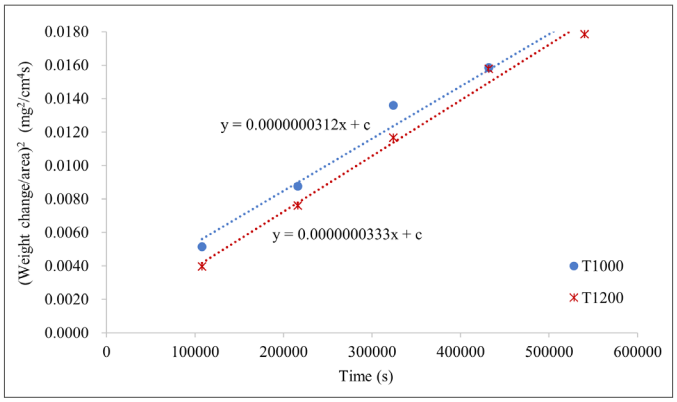

Fig. 3. A square plot of weight change per surface area versus time indicating parabolic rate constant, K_p value

In addition, the T1200 sample with coarse grain size recorded a higher parabolic rate constant, indicating a high rate of oxidation occurred in this sample. If seen from the oxidation kinetics on the red line in Fig. 1, the T1200 sample started with a lower weight change, but started to increase in weight change after 120 hours, indicating that the oxide scale formation was relatively slow at the beginning but it increased as the exposure time increases. It recorded that the T1200 sample had a lower weight change when compared to the T1000 sample from the beginning of the exposure time until the exposure time of 120 hours. However, starting from an exposure time of 120 hours, the weight gain of the T1200 sample began to be rise. This explains why this T1200 sample records a continuous reading of high parabolic rate, where the increase in weight indicates that the oxide layer is still forming.

$$\log x = 1/m \log t + c \quad (1)$$

$$x^2 = K_p t + c \quad (2)$$

3.3. Phase Analysis

The XRD technique was carried out to identify the oxide phase present in the oxidized sample. The XRD peaks for the T1000 sample at 30 and 150 hours are depicted in Figs. 4 and 5, respectively. The T1000 sample presented in this paper, shows a significant peak of both sample in this study. The main noticeable peak is Fe-Ni-Cr alloy base metal at 2 theta 43.9° and 51.1°. A higher intensity of this phase was recorded at 30 hours exposure compared to 150 hours exposure indicating a thin oxide layer formed after 30 hours. The thin oxide layer formed on the surface of this alloy results from the x-ray beam being able to penetrate deep into the base metal, which records the higher intensity of this base metal phase.

On the other hand, the lower intensity peak of Fe-Ni-Cr base metal after 150 hours of exposure indicates that a thicker oxide phase is present on the surface of the sample. Moreover, similar oxide scales are present in both samples T1000 and T1200, recording the existence of a $MnCr_2O_4$ spinal structure, a Cr_2O_3

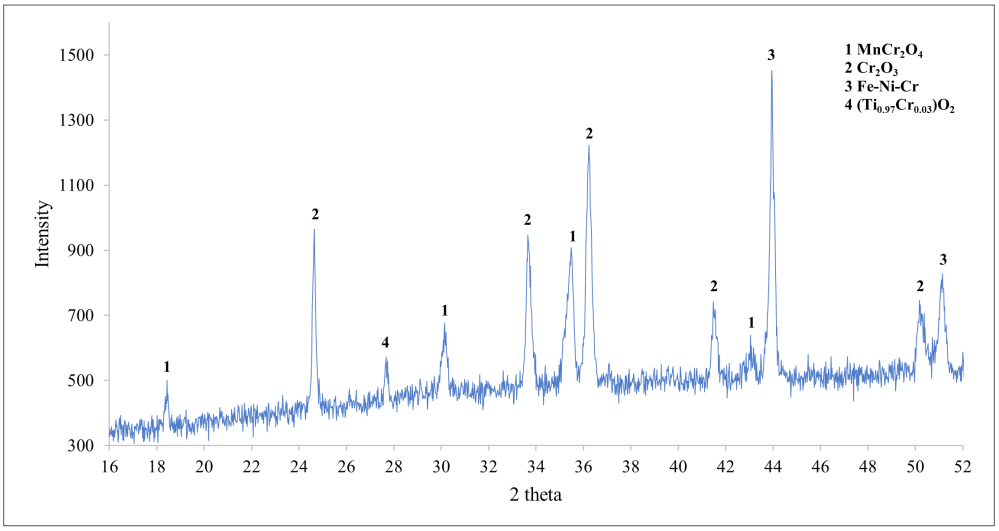

Fig. 4. XRD pattern of T1000 sample subjected to isothermal oxidation at 950°C for 30 h

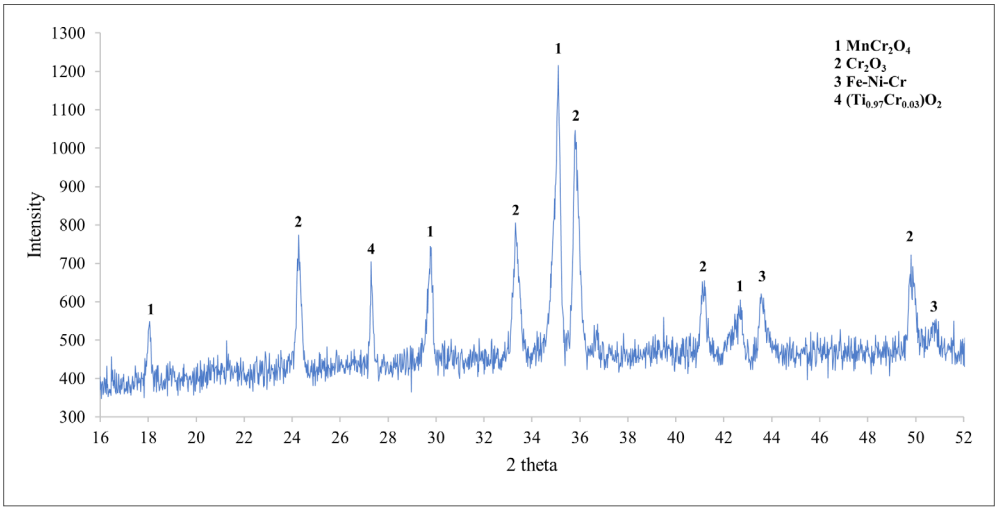

Fig. 5. XRD pattern of T1000 sample subjected to isothermal oxidation at 950°C for 150 h

corundum structure and a$(Ti_{0.97}Cr_{0.03})O_2$ fluorite structure with the addition of Ni-based Fe-Ni-Cr alloy peaks detected as the austenite phase. The establishment of a protective oxide phase containing Mn and Ti elements in the Cr-based oxide phase is desired because the Mn and/or Ti elements can delay the formation of active Cr_2O_3 which can lead to volatilization effects that can diminish the protective behavior of the oxide scale. The establishment of Mn-Cr and Ti-Cr oxides is said to reduce the effect of Cr evaporation, thus increasing the likelihood of oxide exfoliation [3,9,14,28,30].

3.4. Surface morphology

Figs. 6 and 7 show SEM images of T1000 and T1200 samples after 150 hours of exposure, respectively. It can be seen that both samples display a uniform and continual oxide scale developed on the surface of the alloy. The grain boundary oxides are clearly noticeable on the T1200 sample, presented as a network-like structure with a notch shape as shown in Fig. 7. The formation of a network-like structure due to grain boundaries is a short-circuited pathways that contributes to the rapid diffusion of ions through the metal-oxide interface. When rapid ion diffusion occurs, it provides a higher source of metal ions to combine with oxygen ions in the environment to form oxide scale. This mechanism is also contributed by the vertical oxide growth mechanism that thickens the oxide layer. This phenomenon will cause the formation of a notch structure because it forms a thick oxide scale in a localized area at the grain boundary.

On the other hand, the T1000 fine-grained sample produced well-distributed oxides over the entire surface due to smaller grains having adjacent grain boundaries that formed a uniform oxide scale. This uniform oxide structure is contributed by the growth mechanism of uniform vertical oxide and uniform horizontal oxide to form an even oxide layer.

However, sample T1200 displays evidence of oxide exfoliation occurring at grain boundary oxides. This analysis is consistent with the higher parabolic rate constant recorded for

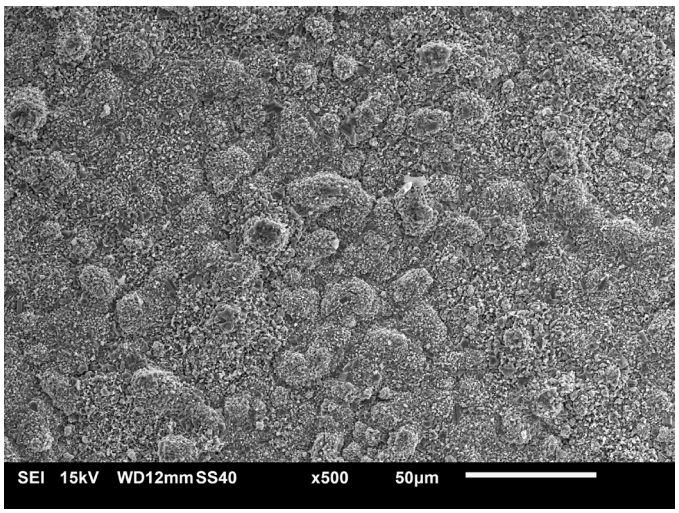

Fig. 6. SEM image of the surface of T1000 sample subjected to isothermal oxidation at 950°C for 150 h

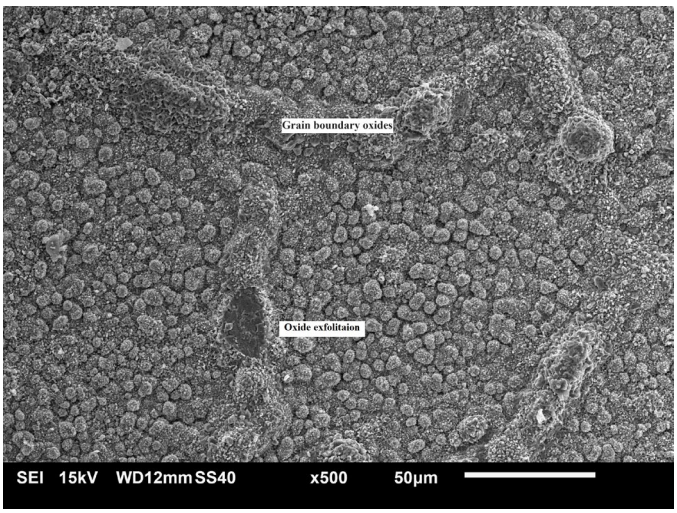

Fig. 7. SEM image of the surface of T1200 sample subjected to isothermal oxidation at 950°C for 150 h

this sample, indicating a higher oxidation rate occurred. Higher oxidation rates will cause uncontrolled oxide scale formation that supposedly protects the base metal. A high oxidation rate will cause the diffusion mechanism to also be high, causing reduced oxide scale adhesion leading to exfoliation.

4. Conclusions

The heat-treated sample T1000 fine grain structure of Ni-based Fe-33Ni-19Cr alloy exhibits good oxidation protection with a uniform oxide layer of lower parabolic rate constant. While the coarse grain T1200 sample showed a higher parabolic rate constant indicating a higher oxidation rate with evidence of oxide exfoliation on the oxidized surface.

Acknowledgments

This research was funded by the Ministry of Higher Education Malaysia under the Fundamental Research Grant Scheme (FRGS) FRGS/1/2020/TK0/UNIMA)/02/43.

REFERENCES

[1] L. Tan, Corrosion Behavior of Ni-Base Alloys for Advanced High Temperature Water-Cooled Nuclear Plants. Corrosion Science **50** (11), 3056-3062 (2008).
DOI: https://doi.org/10.1016/j.corsci.2008.08.024

[2] Z. Zulnuraini, N. Parimin, Isothermal oxidation behavior of Fe-33Ni-18Cr alloy in different heat treatment temperature. Materials Science Forum **1010**, 46-51 (2020).
DOI: https://doi.org/10.4028/www.scientific.net/MSF.1010.46

[3] D. Saber, I.S. Emam, R. Abdel-Karim, High temperature cyclic oxidation of Ni based superalloys at different temperatures in air. Journal of Alloys and Compounds **719**, 133-141 (2017).
DOI: https://doi.org/10.1016/j.jallcom.2017.05.130

[4] M.R. Hawryluk, M. Lachowicz, M. Janik, Z. Gronostajski, M. Stachowicz, Effect of the Heating Temperature of a Nickel-Chromium Steel Charge Material on the Stability of the Forging Process and the Durability of the Die. Arch. Metall. Mater. **68** (2), 711-722 (2023).
DOI: https://doi.org/10.24425/amm.2023.142453

[5] M. Yunus Khan, P. Sudhakar, B.S. Pabla, Investigation of Surface Characteristics of Inconel-625 by EDM with Used Cooking Oil-Based Biodiesel as Dielectric Fluid. Arch. Metall. Mater. **68** (4), 1225-1232 (2023).
DOI: https://doi.org/10.24425/amm.2023.146186

[6] D. Ahmet, C.C. Emre, Microstructural Evolution and Oxidation Behavior of Fe-4Cr-6Ti Ferritic Alloy with Fe2Ti Laves Phase Precipitates. Arch. Metall. Mater. **67** (3), 827-836 (2022).
DOI: https://doi.org/10.24425/amm.2022.139672

[7] K. Krystek, K. Krzanowska, M. Wierzbinska, M. Motyka, The Effect of Selected Process Conditions on Microstructure Evolution of the Vacuum Brazed Joints of Hastelloy X Nickel Superalloy Sheets. Arch. Metall. Mater. **67** (4), 1551-1561 (2022).
DOI: https://doi.org/10.24425/amm.2022.142375

[8] H. Long, S. Mao, Y. Liu, Z. Zhang, X. Han, Microstructural and compositional design of Ni-based single crystalline superalloys – A review. Journal of Alloys and Compounds **743**, 203-220 (2018).
DOI: https://doi.org/10.1016/j.jallcom.2018.01.224

[9] T.D. Nguyen, K. Zhang, D.J. Young, Effect of Mn on oxide formation by Fe-Cr and Fe-Cr-Ni alloys in dry and wet CO2 gases at 650°C. Corrosion Science **112**, 110-127 (2016).
DOI: https://doi.org/10.1016/j.corsci.2016.07.014

[10] R.C. Reed, C.M.F. Rae, Physical Metallurgy of the Nickel-Based Superalloys. Physical Metallurgy (Fifth Edition), 2215-2290 (2014).
DOI: https://doi.org/10.1016/B978-0-444-53770-6.00022-8

[11] G. Dercz, I. Matula, K. Prusik, J. Zajac, M. Szklarska, A. Kazek-Kesik, W. Simka, Effect of Nb and Zr alloying additives on struc-

ture and properties of Ti-Ta-Nb-Zr alloys for medical applications. Arch. Metall. Mater. **68** (3), 1137-1142 (2023).
DOI: https://doi.org/10.24425/amm.2023.145485

[12] C. Yong-Hoon, H. Gi-Su, P. So-Yeon, Effect of Nb and Mo Addition on the Microstructure and Wear Behavior of Fe-Cr-B Based Metamorphic Alloy Coating Layer Manufactured by Plasma Spray Process. Arch. Metall. Mater. **67** (4), 1521-1524 (2022).
DOI: https://doi.org/10.24425/amm.2022.141086

[13] T. Goryczka, G. Dercz, Effect of Milling Time on Crystallization Sequence and Microstructure of Niti Alloys Produced Via High-Energy Ball Milling. Arch. Metall. Mater. **68** (3), 1127-1135 (2023).
DOI: https://doi.org/10.24425/amm.2023.145484

[14] N. Parimin, E. Hamzah, Influence of Ti on Oxide Formation During Isothermal Oxidation of 800H Ni-Based Alloys. Key Engineering Materials **929**, 29-34 (2022).
DOI: https://doi.org/10.4028/p-g4e757

[15] H. Chen, H. Wang, Q. Sun, C. Long, T. Wei, S.H. Kim, J. Chen, C. Kim, C. Jang, Oxidation behavior of Fe-20Cr-25Ni-Nb austenitic stainless steel in high temperature environment with small amount of water vapor. Corrosion Science **145**, 90-99 (2018).
DOI: https://doi.org/10.1016/j.corsci.2018.09.016

[16] J. Jiang, G. Xiao, Y. Wang, Y. Liu, High temperature oxidation behavior of the wrought Ni-based superalloy GH4037 in the solid and semi-solid state. Journal of Alloys and Compounds **784**, 394-404 (2019).
DOI: https://doi.org/10.1016/j.jallcom.2019.01.093

[17] X. Zhuang, Y. Tan, X. You, P. Li, L. Zhao, C. Cui, H. Zhang, H. Cui, High temperature oxidation behavior and mechanism of a new Ni-Co-based superalloy. Vacuum **189**, 110219 (2021).
DOI: https://doi.org/10.1016/j.vacuum.2021.110219

[18] J.W.X. Wo, H.T. Pang, A.S. Wilson, M.C. Hardy, H.J. Stone, The Isothermal Oxidation of a New Polycrystalline Turbine Disk Ni-Based Superalloy at 800C and Its Modification with Pre-oxidation. Metallurgical and Materials Transactions A **54A**, 1946-1960 (2023).
DOI: https://doi.org/10.1007/s11661-022-06896-8

[19] N. Kumar, V.K. Choubey, Comparative Evaluation of Oxidation Resistance of Detonation Gun-Sprayed Al2O3–40%TiO2 Coating on Nickel–Based Superalloys at 800°C and 900°C. High Temperature Corrosion of Materials **99**, 359-373 (2023).
DOI: https://doi.org/10.1007/s11085-023-10157-3

[20] Y.X. Xu, J.T. Lu, W.Y. Li, X.W. Yang, Oxidation behaviour of Nb-rich Ni-Cr-Fe alloys: Role and effect of carbides Precipitates. Corrosion Science **140**, 252-259 (2018).
DOI: https://doi.org/10.1016/j.corsci.2018.05.040

[21] M. Taylor, R. Ding, P. Mignanelli, M. Hardy, Oxidation behaviour of a developmental nickel-based alloy and the role of minor elements. Corrosion Science **196**, 110002 (2022).
DOI: https://doi.org/10.1016/j.corsci.2021.110002

[22] M.P. Taylor, D. Calderwood, T.D. Reynolds, N. Warnken, P.M. Mignanelli, M.C. Hardy, D.M. Collins, Temperature Range of Heating Rate Dependent Reactions Leading to Spinel Formation on a Ni-Based Superalloy. High Temperature Corrosion of Materials **100**, 65-83 (2023).
DOI: https://doi.org/10.1007/s11085-023-10165-3

[23] C.N. Athreya, K. Deepak, D. Kim, B. de Boer, S. Mandal, V.S. Sarma, Role of grain boundary engineered microstructure on high temperature steam oxidation behaviour of Ni based superalloy alloy 617. Journal of Alloys and Compounds **778**, 224-233 (2019).
DOI: https://doi.org/10.1016/j.jallcom.2018.11.137

[24] X. Wang, J.A. Szpunar, Effects of grain sizes on the oxidation behavior of Ni-based alloy 230 and N. Journal of Alloys and Compounds **752**, 40-52 (2018).
DOI: https://doi.org/10.1016/j.jallcom.2018.04.173

[25] Z. Liu, Q. Ding, Q. Zhou, X. Yao, X. Wei, X. Zhao, Y. Wang, Z. Zhang, H. Bei, The effect of oxidation on microstructures of a Ni-based single crystal superalloy during heat-treatment and simulated service conditions. Journal of Materials Science **58**, 6343-6360 (2023).
DOI: https://doi.org/10.1007/s10853-023-08412-8

[26] L. Li, L. Wang, Z. Liang, J. He, J. Qiu, F. Pyczak, M. Song, Effects of Ni and Cr on the high-temperature oxidation behavior and mechanisms of Co- and CoNi-base superalloys. Materials & Design **224**, 111291 (2022).
DOI: https://doi.org/10.1016/j.matdes.2022.111291

[27] Y.X. Xu, J.T. Lu, X.W. Yang, J.B. Yan, W.Y. Li, Effect and role of alloyed Nb on the air oxidation behaviour of Ni-Cr-Fe alloys at 1000°C. Corrosion Science **127**, 10-20 (2017).
DOI: http://dx.doi.org/10.1016/j.corsci.2017.08.003

[28] L. Tan, X. Ren, K. Sridharan, T.R. Allen, Effect of Shot-Peening on the Oxidation of Alloy 800H Exposed to Supercritical Water and Cyclic Oxidation. Corrosion Science **50** (7), 2040-2046 (2008).
DOI: https://doi.org/10.1016/j.corsci.2008.04.008

[29] N. Parimin, E. Hamzah, Effect of Solution Treatment Temperature on the Microstructure of Fe-33Ni-19Cr Alloy. Materials Science Forum **1010**, 21-27 (2020).
DOI: https://doi.org/10.4028/www.scientific.net/MSF.1010.21

[30] A. Col, V. Parry, C. Pascal, Oxidation of a Fe-18Cr-8Ni austenitic stainless steel at 850°C in O2: Microstructure evolution during breakaway oxidation, Corrosion Science **114**, 17-27 (2017).
DOI: https://doi.org/10.1016/j.corsci.2016.10.029